Lie group analysis of radiation natural convection heat transfer past an inclined porous surface

J. Lee[1,*], P. Kandaswamy[1], M. Bhuvaneswari[2] and S. Sivasankaran[2]

[1]*School of Mechanical Engineering, Yonsei University, Seoul 120 749, South Korea*
[2]*Department of Mechanical Engineering, National Cheng Kung University, Tainan 70701, Taiwan*

Abstract

Natural convection heat transfer fluid flow past an inclined plate embedded in a fluid-saturated porous medium is investigated by Lie group analysis. The governing partial differential equations are reduced to a system of ordinary differential equations by the scaling symmetries. From numerical results, it is found that the thermal and momentum boundary layer thicknesses are increased as the radiation parameter is increased. Also, it is observed that the velocity is increased and the temperature is decreased for increasing the buoyancy parameter and the porosity parameter.

---

1. Introduction

In recent years, convection heat transfer from surfaces embedded in porous media has received considerable attention because of its wide range of applications, such as geothermal systems, petroleum processes, water purification, ground water pollution, industrial filtration, ceramic engineering, solid matrix heat exchangers, storage of grain, fruits and vegetables and the storage of nuclear waste.

In this paper, symmetry methods are applied to a natural convection boundary layer problem. The main advantage of such methods is that they can successfully be applied to non-linear differential equations. The symmetries of differential equations are continuous groups of transformations. Differential equations are remaining invariant under these transformations. The symmetry solutions are quite popular because they result in the reduction of the number of independent variables of the problem.

Effect of porosity on the free convection flow along a vertical plate embedded in a porous medium was

investigated by Beithou *et al*. [1]. Their results show that as the porosity is increased the temperature variation becomes steeper, that is, the heat transfer rate is increased. Chen [2] studied the natural convection flow over a permeable inclined surface with variable wall temperature and concentration. The results show that the velocity is decreased in the presence of a magnetic field. Increasing the angle of inclination decreases the effect of buoyancy force. Heat transfer rate is increased when the Prandtl number is increased. Duwairi [3], who investigated the effect of viscous and Joule heating on forced convection flow from radiative isothermal surfaces found that the heat transfer rate is decreased as the radiation parameter is increased. Radiative and magnetic effects on free convection and mass-transfer flow past a flat plate were studied by Ibrahim *et al*. [4]. They obtained similarity reductions and found analytical and numerical solutions using scaling symmetry. Kalpadides and Balassas [5] also studied the free convective boundary layer problem using Lie group analysis.

Kandaswamy *et al*. [6] studied the convection flow of an incompressible viscous electrically conducting fluid in a porous medium. They showed that an in-

---
*Corresponding author. Tel.: +82 2 2123 2816, Fax.: +82 2 312 2159
E-mail address: jinholee@yonsei.ac.kr

crease in the magnetic parameter retards the flow and an increase in the porosity parameter accelerates the flow. Kumari *et al*. [7] investigated the mixed convection flow over a vertical wedge embedded in a porous medium. They found that the heat transfer is increased with the Prandtl number and the effect of permeability on the heat transfer is very small. Lai and Kulacki [8] studied the convection from horizontal impermeable surfaces in saturated porous medium. It is observed that the inertial term has a pronounced effect on the flow for higher values of parameter by the inertial effect on natural convection. Shu and Pop [9] numerically studied the natural convection from inclined wall plumes in a porous medium. The velocity is increased while the temperature is decreased with increasing the tilting angle. Yurusoy and Pakdemirli [10] studied the boundary layer equations for Newtonian / non-Newtonian fluids by using Lie group method. So far no attempt has been made to study the radiative heat transfer in a porous medium using Lie groups, and hence we study the problem of radiative natural convection heat transfer flow past an inclined surface embedded in a porous medium for various parameters using Lie groups.

2. Mathematical analysis

Consider the heat transfer by natural convection in laminar boundary layer flow of an incompressible viscous fluid along an inclined surface embedded in a fluid-saturated porous medium with an acute angle α from the vertical. The surface is maintained at a constant temperature T_w which is higher than the constant temperature $T\infty$ of the surrounding fluid. The fluid properties are assumed to be constant. The governing equations of the mass, momentum and energy for the steady flow can be written as,

$$\frac{\partial u}{\partial x} + \frac{\partial v}{\partial y} = 0, \tag{1}$$

$$u\frac{\partial u}{\partial x} + v\frac{\partial u}{\partial y} = \nu\frac{\partial^2 u}{\partial y^2} + g\beta(T - T_\infty)\cos\alpha - \frac{\nu}{k'}u, \tag{2}$$

$$u\frac{\partial T}{\partial x} + v\frac{\partial T}{\partial y} = \frac{k}{\rho c_p}\frac{\partial^2 T}{\partial y^2} - \frac{\lambda}{k}\frac{\partial q_r}{\partial y}, \tag{3}$$

with the boundary conditions

$$u = v = 0, \quad T = T_w, \quad \text{at } y = 0,$$
$$u = 0, \quad T = T_\infty, \quad \text{as } y \to \infty, \tag{4}$$

where *u* and *v* are the velocity components; *x* and *y* are the space coordinates; *T* is the temperature; *v* is the kinematic viscosity of the fluid; *g* is the acceleration due to gravity; *β* is the coefficient of thermal expansion *λ* is the thermal diffusivity; q_r is the local radiative heat flux; *k* is the thermal conductivity of fluid; *ρ* is the density of the fluid; c_p is the specific heat of the fluid; k' is the permeability of the porous medium and *α* is the angle of inclination.

The radiative heat flux term is simplified by using the Rosseland approximation in Sparrow and Cess [11],

$$q_r = -\frac{4\sigma_o}{3k^*}\frac{\partial T^4}{\partial y} \tag{5}$$

where σ_o and k^* are the Stefan-Boltzmann constant and mean absorption coefficient respectively.

We assume that the temperature differences within the flow are sufficiently small such that T^4 may be expressed as a linear function of the temperature. This is accomplished by expanding T^4 in a Taylor series about T_∞ and neglecting higher-order terms, thus

$$T^4 \cong 4T_\infty^3 T - 3T_\infty^4. \tag{6}$$

The nondimensional variables are

$$\bar{x} = \frac{x}{L}, \qquad \bar{y} = \frac{y}{L}, \qquad \bar{u} = \frac{uL}{\nu},$$
$$\bar{v} = \frac{vL}{\nu}, \qquad \theta = \frac{T - T_\infty}{T_w - T_\infty} \tag{7}$$

where $\bar{u}$ and $\bar{v}$ are the dimensionless velocity components; $\bar{x}$ and $\bar{y}$ are the dimensionless space coordinates; *L* is the characteristic length; and *θ* is the dimensionless temperature.

Substituting (5)-(7) into equations (1)-(4) and dropping the over bars, we obtain,

$$\frac{\partial u}{\partial x} + \frac{\partial v}{\partial y} = 0 \tag{8}$$

$$u\frac{\partial u}{\partial x} + v\frac{\partial u}{\partial y} = \frac{\partial^2 u}{\partial y^2} + Gr\theta\cos\alpha - \frac{1}{K}u \tag{9}$$

$$u\frac{\partial \theta}{\partial x} + v\frac{\partial \theta}{\partial y} = \frac{1}{Pr}(1 + 4R)\frac{\partial^2 \theta}{\partial y^2} \tag{10}$$

with the boundary conditions

$$u = v = 0, \quad \theta = 1, \quad \text{at } y = 0,$$
$$u = 0, \quad \theta = 0, \quad \text{as } y \to \infty, \quad (11)$$

where $Gr = \dfrac{g\beta(T_w - T_\infty)L^3}{\nu^2}$ is the Grashof number,

$\text{Pr} = \dfrac{\rho \nu c_p}{k}$ is the Prandtl number, $K = \dfrac{k'}{L^2}$ is

the dimensionless permeability parameter and

$R = \dfrac{4\sigma_o T_\infty^3}{3kk*}$ is the radiation parameter.

3. Symmetry groups of equations

The symmetry groups of equations (8)-(10) are calculated by using the classical Lie group approach in Bluman and Kumei [12]. The one-parameter infinitesimal Lie group of transformations leaving (8)-(10) invariant is defined as

$$x^* = x + \varepsilon \xi_1(x, y, u, v, \theta)$$
$$y^* = y + \varepsilon \xi_2(x, y, u, v, \theta)$$
$$u^* = u + \varepsilon \eta_1(x, y, u, v, \theta) \quad (12)$$
$$v^* = v + \varepsilon \eta_2(x, y, u, v, \theta)$$
$$\theta^* = \theta + \varepsilon \eta_3(x, y, u, v, \theta)$$

The corresponding generator X is defined as

$$X = \xi_1 \frac{\partial}{\partial x} + \xi_2 \frac{\partial}{\partial y} + \eta_1 \frac{\partial}{\partial u} + \eta_2 \frac{\partial}{\partial v} + \eta_3 \frac{\partial}{\partial \theta} \quad (13)$$

The total derivative operator is

$$D_i = \frac{\partial}{\partial x_i} + u_i^\mu \frac{\partial}{\partial u^\mu} + u_{ij}^\mu \frac{\partial}{\partial u_j^\mu} + \cdots$$
$$+ u_{i,i_1,i_2,\cdots i_n}^\mu \frac{\partial}{\partial u_{i_1,i_2,\cdots i_n}^\mu} + \cdots \quad (14)$$

with summation over a repeated index.

$$\eta_1^{(1)1} + \eta_2^{(1)2} = 0$$
$$\eta^1 u_1 + u\eta_1^{(1)1} + \eta^2 u_2 + v\eta_2^{(1)1}$$
$$= \eta_{22}^{(2)1} + Gr\eta^3 \cos\alpha - \frac{1}{K}\eta^1 \quad (15)$$
$$\eta^1 \theta_1 + u\eta_1^{(1)3} + \eta^2 \theta_2 + v\eta_2^{(1)3} = \frac{1}{\text{Pr}}(1 + 4R)\eta_{22}^{(2)3}$$

The invariance condition in Bluman and Kumei (1989) becomes
where,

$$\eta_1^{(1)1} = D_1\eta^1 - (D_1\xi_1)u_1 - (D_1\xi_2)u_2$$
$$\eta_2^{(1)1} = D_2\eta^1 - (D_2\xi_1)u_1 - (D_2\xi_2)u_2$$
$$\eta_2^{(1)2} = D_2\eta^2 - (D_2\xi_1)v_1 - (D_2\xi_2)v_2$$
$$\eta_1^{(1)3} = D_1\eta^3 - (D_1\xi_1)\theta_1 - (D_1\xi_2)\theta_2 \quad (16)$$
$$\eta_2^{(1)3} = D_2\eta^3 - (D_2\xi_1)\theta_1 - (D_2\xi_2)\theta_2$$
$$\eta_{22}^{(2)1} = D_2\eta_2^{(1)1} - (D_2\xi_1)u_{21} - (D_2\xi_2)u_{22}$$
$$\eta_{22}^{(2)3} = D_2\eta_2^{(1)3} - (D_2\xi_1)\theta_{21} - (D_2\xi_2)\theta_{22}$$

Substituting (14) and (16) into (15) and then eliminating v_2, u_{22} and θ_{22} through substitution of (8),(9) and (10), and solving we obtain the infinitesimals as

$$\xi_1 = c_1 x - c_2$$
$$\xi_2 = -\alpha(x)$$
$$\eta_1 = c_1 u$$
$$\eta_2 = u\alpha'(x) \quad (17)$$
$$\eta_3 = c_1\theta \ .$$

Imposing the restrictions from boundaries and from the boundary conditions on the infinitesimals, we obtain the following form for equations (17):

$$\xi_1 = c_1 x - c_2$$
$$\xi_2 = 0$$
$$\eta_1 = c_1 u$$
$$\eta_2 = 0 \quad (18)$$
$$\eta_3 = c_1\theta \ ,$$

where the parameter c_1 represents the scaling transformation and parameter c_2 represents translation in the x coordinate.

4. Reduction to ordinary differential equations

In this section, parameter c_1 is taken to be arbitrary and all other parameters are zero in (18).
The characteristic equations are

$$\frac{dx}{x} = \frac{dy}{0} = \frac{du}{u} = \frac{dv}{0} = \frac{d\theta}{\theta} \quad (19)$$

from which the similarity variables, the velocities and temperature turn out to be of the form

$$\eta = y, \quad u = xF_1(\eta), \quad v = F_2(\eta), \quad \theta = xF_3(\eta). \tag{20}$$

Substituting (20) into equations (8)-(11), we finally obtain the system of nonlinear ordinary differential equations

$$F_1'' = F_1^2 + F_2F_1' - GrF_3\cos\alpha + \frac{1}{K}F_1$$
$$F_2' = -F_1 \tag{21}$$
$$F_3'' = \frac{Pr}{1+4R}(F_2F_3' + F_1F_3)$$

The appropriate boundary conditions are expressed as

$$\begin{aligned}
F_1 &= F_2 = 0, \quad F_3 = 1 \quad at \quad \eta = 0, \\
F_1 &= 0, \quad\quad\quad F_3 = 0, \quad as \quad \eta \to \infty. \tag{22}
\end{aligned}$$

5. Numerical methods for solutions

Since the equations are highly nonlinear, a numerical treatment would be more appropriate. The system of transformed equations (21) together with the boundary conditions (22) is numerically solved by employing a fourth order Runge-Kutta method and Shooting techniques with a systematic guessing of $F_1(0)$ and $F_3(0)$. The procedure is repeated until we get the results up to the desired degree of accuracy, namely 10^{-5} and solutions are presented graphically.

6. Results and discussions

Numerical solutions are obtained for various values of the Prandtl number, Grashof number, the porosity parameter and the radiation parameter. Prandtl number *Pr* is varied from *0.1* to *13.67*, Grashof number *Gr* from *1.0* to *4.0*, the porosity parameter *K* from *2* to *10* and the radiation parameter *R* from *0* to *10* with the angle of inclination α taking the values 0°, 30° and 45°. The numerical results are depicted graphically in the form of velocity and temperature profiles. Most of the investigations are carried out for $\alpha = 45^o$. Some results are taken for $\alpha = 0^o$ (vertical plate case) and 30°.

Fig. 1 (a and b) shows the velocity and temperature profiles for various values of the radiation parameter with *Pr=0.71* (air), *Gr=1*, *K=5*. The velocity and temperature distributions increase with increase in the radiation parameter. It is noted that the temperature

profile approaches a linear shape for high value of the radiation parameter. Increasing the Prandtl number to *13.67*, the velocity and temperature behavior along the boundary layer are displayed in Fig. 2 (a and b). It is found from Fig. 2(a) that the velocity distribution is increased as the radiation parameter (*R = 1,2,5* and *10*) is increased in the region $y \in [0,15]$. The velocity becomes maximum near the surface and finally approaches zero. Increasing the radiation parameter increases both the momentum and thermal boundary layer thicknesses. The velocity and temperature profiles for different Grashof numbers with *Pr=0.71, R=1* and *K=2* are shown in Fig. 3 (a and b). It is found that the velocity is increased rapidly and falls near the boundary due to favorable buoyancy force. The thermal boundary layer thickness is decreased with increasing the buoyancy parameter.
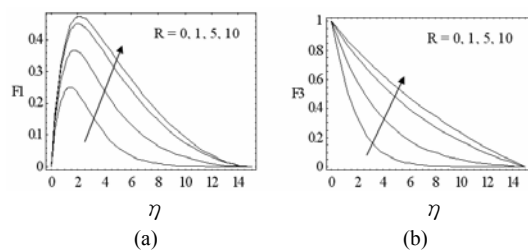

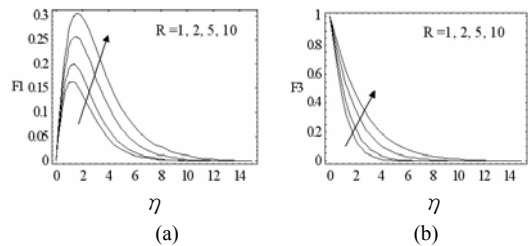Fig. 1. The velocity and temperature profiles for Pr = 0.71, Gr =1 and K=5.

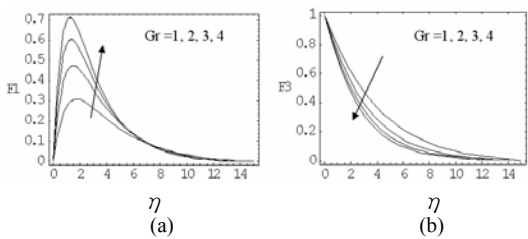Fig. 2. The velocity and temperature profiles for Pr = 13.67, Gr =1 and K=5.

Fig. 3. The velocity and temperature profiles for Pr = 0.71, R =1 and K=2.

The effect of the Prandtl number on the velocity and temperature distributions is presented in Fig. 4 (a and b). It is clear that the velocity is decreased with increasing the Prandtl number. The thermal boundary layer thickness is decreased with increase in the Prandtl number. For low Prandtl number fluids, the temperature profile becomes linear. The reason for such a behavior is that the higher Prandtl number fluid has a relatively low thermal conductivity. This results in the reduction of the thermal boundary layer thickness. It is also observed that the effect of the Prandtl number is to retard the flow. Fig. 5 (a and b) presents the effect of the porosity parameter on the velocity and temperature profiles for $Gr = R = 1$ and $Pr = 0.71$. There are very small changes that occur in both momentum and thermal boundary layers when changes are made in the porosity parameter. The velocity is increased with increase in the porosity parameter. But the temperature is decreased on increasing the porosity parameter. It is only in the pure convection dominated situations that both shear layer (boundary layer in F1) and thermal boundary layer (boundary layer for F2) have similar behavior but in situations where the heat transfer is either conduction dominated or radiation dominated as in the present study the boundary layers for the flow and temperature behave differently. In the present case it is radiation-dominated heat transfer and there is only shear layer and there is no thermal boundary layer.
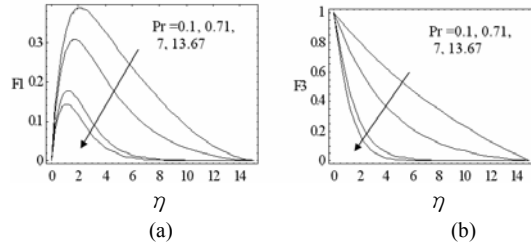
The effect of inclination of the surface for different parameters is depicted in Figs. 6 and 7. For a fixed value of the porosity parameter the velocity is decreased with inclination angles as shown in Fig. 6. The fluid has higher velocity when the surface is vertical than when inclined because the buoyancy effect decreases due to gravity components $g\cos\alpha$ as the plate is inclined. For a fixed value of porosity parameter, the fluid has higher temperature when $\alpha = 30^{\circ}$. Increasing the porosity parameter increases the temperature of the fluid along the surface. The inclination angle $\alpha = 30^{\circ}$ gives the enhanced heat distribution of the convective fluid. Fig. 7 shows the effect of inclination of the surface for different values of the radiation parameter. At a particular angle of inclination, the temperature and the thickness of the thermal boundary layer are increased with increasing the radiation parameter. In the case of radiation-dominated flow and heat transfer the orientation of the gravity has telling effect on the flow and not on temperature since the change in temperature is primarily by radiation and not convection; hence little effect is noticed in the temperature field (F3) in the regular order 0, 30,45 and the flow field (F1) is more dependent on the orientation of the gravity and is in the order 0,45,30.

Fig. 4. The velocity and temperature profiles for Gr = 1, R =1 and K=2.

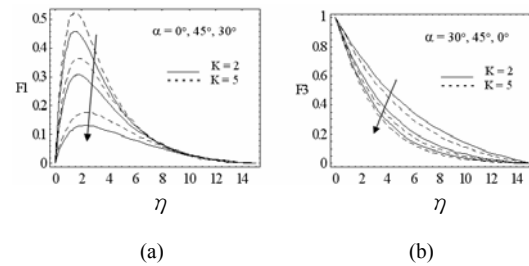Fig. 5. The velocity and temperature profiles for Gr = 1, R =1 and Pr=0.71.

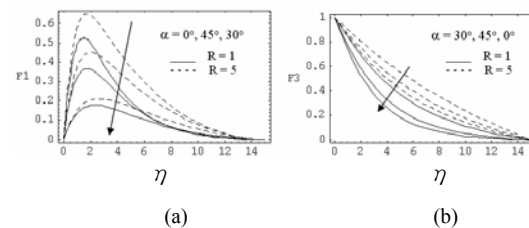Fig. 6. The velocity and temperature profiles for Gr =1, R =1 and Pr=0.71.

Fig. 7. The velocity and temperature profiles for Gr = 1, K =5 and Pr=0.71.

7. Conclusions

Symmetries are obtained for the governing system of partial differential equations, which are reduced to ordinary differential equations. From the numerical results, it is found that the thermal and momentum boundary layer thicknesses increase by increasing the radiation parameter. Increasing Prandtl number decreases both temperature and velocity in the boundary layer. Velocity increases and temperature decreases by increasing Grashof number and the porosity parameter

References

[1] N. Beithou, K. Albayrak and A. Abdulmajeed, Effects of porosity on the free convection flow of non-Newtonian fluids along a vertical plate embedded in a porous medium, *Tr. J. Engg. Env. Sci* 22 (1998) 203-209.

[2] C. H. Chen, Heat and mass transfer in MHD flow by natural convection from a permeable, inclined surface with variable wall temperature and concentration, *Acta Mechanica*, 172 (2004) 219-235.

[3] H. M. Duwairi, Viscous and joule heating effects on forced convection flow from radiate isothermal porous surfaces, *Int. J. Num. Methods Heat Fluid Flow*, 15 (5) (2005) 429-440.

[4] F. S. Ibrahim, M. A. Mansour and M. A. A. Hamad, Lie-group analysis of radiative and magnetic field effects on free convection and mass transfer flow past a semi-infinite vertical flat plate, *Electronic J. Differential Equations* 39 (2005) 1-17.

[5] V. K. Kalpakides and K. G. Balassas, Symmetry groups and similarity solutions for a free convective boundary-layer problem, *Int. J. Non-linear Mech.*, 39 (2004) 1659-1670.

[6] P. Kandaswamy, R. J. Mallakal and L. Debnath, Hydromagnetic free convective flow in A, porous medium, *Engg. Simulation*, 16 (1994) 74-79.

[7] M. Kumari, H. S. Takhar and G. Nath, Mixed convection flow over a vertical wedge embedded in a highly porous medium, *Heat Mass Transfer*, 37 (2001) 139-146.

[8] F. C. Lai and F. A. Kulacki, Non-Darcy convection from horizontal impermeable surfaces in saturated porous media, *Int. J. Heat Mass Transfer*, 30 (10) (1994) 2189-2192.

[9] J. J. Shu and I. Pop, Inclined wall plumes in porous media, *Fluid Dyn. Res*. 21 (1997) 303-317.

[10] M. Yurusoy and M. Pakdemirli, Symmetry reductions of unsteady three-dimensional boundary layers of some non-Newtonian Fluids, *Int. J. Engg. Sci*. 35 (8) (1997) 731-740.

[11] E. M. Sparrow and D. R. Cess, Radiation heat transfer, Augmented Edition, Hemisphere Publishers, Washington DC (1978).

[12] G. W. Bluman and S. Kumei, Symmetries and Differential Equations, Springer, New York, (1989).